Stabilization of Ca^{2+}-permeable AMPA receptors at perisynaptic sites by GluR1-S845 phosphorylation

Kaiwen He[a,b], Lihua Song[a], Laurel W. Cummings[a], Jonathan Goldman[b], Richard L. Huganir[c,1], and Hey-Kyoung Lee[a,b,1]

[a]Department of Biology, College of Chemical and Life Sciences and [b]Neuroscience and Cognitive Science (NACS) Program, University of Maryland, College Park, MD 20742; and [c]Solomon H. Snyder Department of Neuroscience, Howard Hughes Medical Institute, Johns Hopkins School of Medicine, Baltimore, MD 21210

Contributed by Richard L. Huganir, September 25, 2009 (sent for review July 23, 2009)

AMPA receptor (AMPAR) channel properties and function are regulated by its subunit composition and phosphorylation. Certain types of neural activity can recruit Ca^{2+}-permeable (CP) AMPARs, such as GluR1 homomers, to synapses likely via lateral diffusion from extrasynaptic sites. Here we show that GluR1-S845 phosphorylation can alter the subunit composition of perisynaptic AMPARs by providing stability to GluR1 homomers. Using mice specifically lacking phosphorylation of the GluR1-S845 site (GluR1-S845A mutants), we demonstrate that this site is necessary for maintaining CP-AMPARs. Specifically, in the GluR1-S845A mutants, CP-AMPARs were absent from perisynaptic locations mainly due to lysosomal degradation. This regulation was mimicked by acute desphosphorylation of the GluR1-S845 site in wild-type mice by NMDA application. Furthermore, long-term depression (LTD) was associated with a reduction in perisynaptic CP-AMPAR levels. Our findings suggest that GluR1-S845 is necessary for maintaining CP-AMPARs on the surface, especially at perisynaptic sites, and suggest that the regulation of these receptors is involved in synaptic plasticity.

excitatory synaptic transmission | GluR1 homomer

Regulation of AMPA receptor (AMPAR) function is critical for excitatory synaptic function in the brain (1). The majority of synaptic AMPARs are impermeable to Ca^{2+} due to the presence of the GluR2 subunits, which undergo RNA editing at the Q/R site within the pore loop (2). Recent evidence suggests that many forms of synaptic plasticity are associated with changes in the subunit composition of synaptic AMPARs, especially at the level of regulating the GluR2 lacking CP-AMPARs (3). Several studies support the regulation of GluR2 as a mechanism for activity-dependent alterations in synaptic AMPAR subunit composition. For example, CP-AMPAR plasticity (CARP) in cerebellar stellate cells is associated with synaptic incorporation of GluR2-containing AMPARs dependent on interaction with Pick1 (4, 5). Similarly, the appearance of CP-AMPARs at synapses by ischemia (6) or cocaine injection (7) is dependent on GluR2-Pick1 interaction. However, the appearance of synaptic CP-AMPARs under various in vitro and in vivo synaptic plasticity paradigms is often associated with an increase in the GluR1 subunit with little change in the GluR2 levels (8–12), implicating a GluR1-dependent mechanism.

Previously, we found that experience-dependent appearance of CP-AMPARs in visual cortex correlates with an increase in the phosphorylation of S845 on the GluR1 subunit (9). GluR1-S845 is a substrate of protein kinase A (PKA) (13), which when phosphorylated enhances channel mean open probability (14) and promotes synaptic trafficking of GluR1-containing AMPARs (15, 16), especially to extrasynaptic sites (16–18). To examine whether GluR1-S845 phosphorylation plays a role in regulating AMPAR subunit composition, we performed a series of experiments using a line of mutant mice specifically lacking the S845 site (GluR1-S845A mutants) (19). Here we provide evidence supporting the hypothesis that S845 phosphorylation regulates perisynaptic AMPAR subunit composition by stabilizing GluR1 homomers, and that LTD is associated with the removal of CP-AMPARs.

Results

CP-AMPARs at Perisynaptic Sites of Schaffer Collateral Inputs to CA1. Using the property that CP-AMPARs are sensitive to application of an exogenous polyamine philanthotoxin-433 (PhTX), we tested the presence of these receptors at Schaffer collateral synapses on CA1 neurons. Similar to previous reports (20, 21), bath application of PhTX (3 μM) did not alter AMPAR responses measured extracellularly in the presence of 100 μM DL-APV (102 $\pm$ 2.6% of baseline at 60 min post-PhTX, $n = 7$) (Fig. 1*A*). However, when synaptic responses were probed using paired-pulses of 50 ms interstimulus interval (ISI), PhTX significantly depressed AMPAR responses (84 $\pm$ 2.2% of baseline at 60 min post-PhTX, $n = 18$; $P < 0.016$, paired t-test) (Fig. 1*A*) without altering the paired-pulse ratio (baseline = 1.74 $\pm$ 0.04, post-PhTX = 1.78 $\pm$ 0.05, $n = 18$, $P = 0.14$, paired t-test). These results suggest that paired-pulse (PP) stimulation reveals CP-AMPARs unlike conventional single-pulse (SP) stimulation. To test whether this is due to activation of perisynaptic receptors, we examined the effect of PhTX on hippocampal slices treated with 10 μM TBOA, an inhibitor of glutamate transporters, which allows spill-over of glutamate. In the presence of TBOA, PhTX caused a significant reduction in AMPAR synaptic responses with SP stimulation (83 $\pm$ 4.4% of baseline at 60 min post-PhTX, $n = 8$; $P < 0.005$, paired t-test) (Fig. 1*A*), similar to when using PP stimulation.

Because the polyamine sensitivity of CP-AMPARs is voltage-dependent (22, 23), an alternative explanation for the action of TBOA is that it induces glutamate accumulation at synapses to enhance postsynaptic depolarization, which then permits the detection of synaptic CP-AMPARs. To investigate this, we performed whole-cell voltage clamp experiments using SP stimulations. Bath application of TBOA while holding the cells at -70 mV significantly increased the AMPAR-EPSC amplitude (130 $\pm$ 13.0% of baseline at 15 min post-TBOA, $n = 11$; $P < 0.003$, paired t-test) (Fig. 1B_1). This suggests that blocking glutamate transporters recruit additional AMPARs, likely perisynaptic as the decay time constant (τ) of AMPAR-EPSCs was also increased (pre-TBOA: 7.6 $\pm$ 0.32 ms; post-TBOA: 8.2 $\pm$ 0.34 ms; $n = 11$, $P < 0.02$, paired t-test). After the responses stabilized in the presence of TBOA, we bath applied PhTX,

Author contributions: K.H. and H.-K.L. designed research; K.H., L.S., L.W.C., and J.G. performed research; R.L.H. contributed new reagents/analytic tools; K.H., L.S., and L.W.C. analyzed data; and K.H. and H.-K.L. wrote the paper.

Conflict of interest statement: Under a licensing agreement between Millipore Corporation and The Johns Hopkins University, R.L.H. is entitled to a share of royalties received by the University on sales of products described in this article. R.L.H. is a paid consultant to Millipore Corporation.

[1]To whom correspondence may be addressed. E-mail: rhuganir@jhmi.edu or hlee21@umd.edu.

This article contains supporting information online at www.pnas.org/cgi/content/full/0910338106/DCSupplemental.

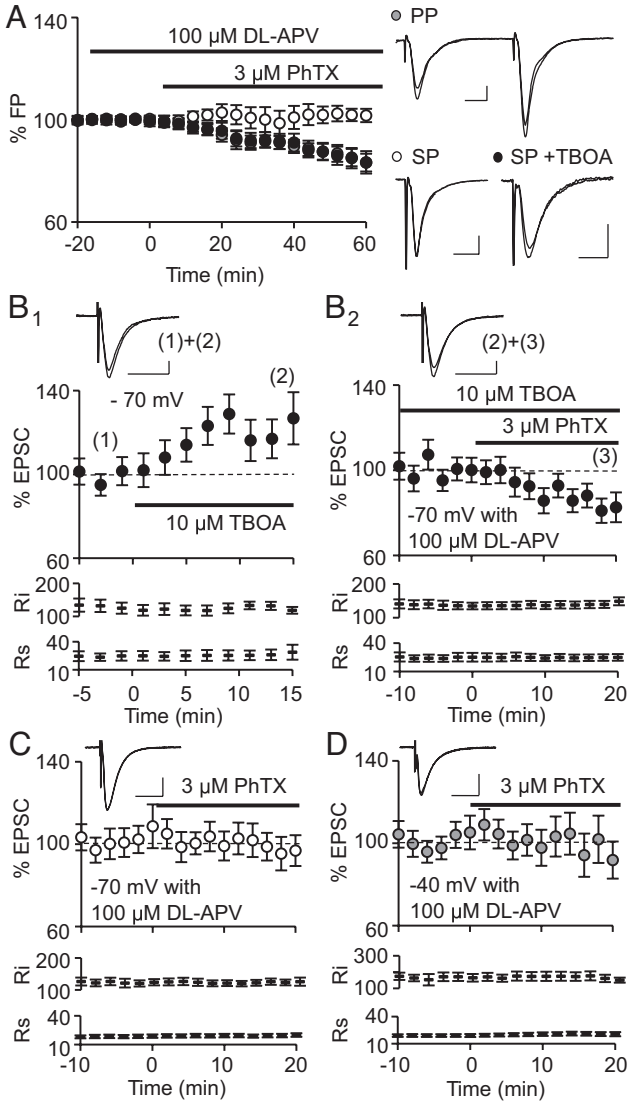

Fig. 1. Detection of perisynaptic CP-AMPARs at Schaffer Collateral inputs to CA1. (*A*) Left: PhTX (3 μM) depressed AMPAR-mediated field potentials (FPs) evoked by paired-pulse (PP) stimulation (50 ms ISI, gray circles), but not by single-pulse (SP) stimulation (open circles). Ten micromolar TBOA treatment revealed PhTX sensitivity with SP stimulation (black circles). Right: Superimposed traces taken during baseline and 1 h post-PhTX. (Scale bar, 0.25 mV, 10 ms.) (B_1) TBOA potentiated AMPAR-EPSC. (B_2) PhTX depressed SP evoked AMPAR-EPSCs in the presence of TBOA. Insets: Superimposed AMPAR-EPSC traces taken at times indicated. (*C*) PhTX had no effect on SP evoked AMPAR-EPSC when voltage clamped at −70 mV. (*D*) PhTX had no effect on SP evoked AMPAR-EPSC when cells are depolarized to −40 mV. (*C, D*) Insets: Superimposed EPSC traces taken at baseline and 20 min post-PhTX. (*B–D*) Bottom panels: Input resistance (Ri) and series resistance (Rs) in MΩ. (Scale bar, 25 pA, 20 ms.)

which caused a significant decrease in AMPAR-EPSC amplitude (81 ± 8.0% of renormalized baseline at 20 min post-PhTX, $n = 12$; $P < 0.001$, paired t-test) (Fig. 1B_2). PhTX in the presence of TBOA also further increased the decay kinetics (τ) of AMPAR-EPSCs (pre-PhTX: 8.6 ± 0.45 ms; post-PhTX: 9.3 ± 0.50 ms; $n = 12$; $P < 0.001$, paired t-test) consistent with the idea of blocking CP-AMPARs with shorter decay kinetics (24). AMPAR-EPSCs did not change when PhTX was applied without TBOA (97 ± 7.5% of baseline at 20 min post-PhTX, $n = 13$) (Fig. 1*C*) or when PhTX was applied alone, while depolarizing the cells to −40 mV (92 ± 9.0%, $n = 10$) (Fig. 1*D*). Collectively, our data support the idea that CP-AMPARs are located perisynaptically.

GluR1-S845 Phosphorylation Plays a Role in Maintaining Perisynaptic CP-AMPARs. Next we examined how CP-AMPARs are maintained at perisynaptic sites. We previously found that the phosphorylation status of GluR1-S845 correlates with the appearance of CP-AMPARs at visual cortex synapses when rodents are deprived of vision (9). GluR1-S845 is a PKA site (13), which plays a critical role in bidirectional synaptic plasticity (25, 26). One proposed mechanism is that phosphorylation of GluR1-S845 "primes" the AMPARs for synaptic delivery (16, 19), and stabilizes surface AMPARs (18, 26–28). To test the hypothesis that GluR1-S845 phosphorylation is involved specifically in stabilizing the CP-AMPARs at perisynaptic sites, we used a line of mutant mice lacking the GluR1-S845 site (GluR1-S845A mutants) (19).

We first examined whether CP-AMPARs are present at perisynaptic sites in the GluR1-S845A homozygous (HM) mice by probing the synapses using the PP stimulation (ISI = 50 ms). In contrast to wild-types (Fig. 1*A*), GluR1-S845A HM lacked PhTX sensitivity of AMPAR responses (103 ± 2.7% of baseline at 60 min post-PhTX, $n = 8$) (Fig. 2*A*). Phosphorylation of GluR1-S845 also regulates the mean open probability of AMPAR channels (14), which could have prevented the detection of perisynaptic CP-AMPARs in the mutants. To rule this out, we increased the current through AMPAR channels in the GluR1-S845A HM by removing AMPAR desensitization using cyclothiazide (CTZ) (29). Bath application of 50 μM CTZ increased both the amplitude and the duration of AMPAR responses (Fig. 2*A*) resulting in about 1.6-fold increase in the total charge transfer (measured as the integrated area of AMPAR response). However, a subsequent application of 3 μM PhTX during PP stimulation failed to alter AMPAR responses in the mutants (Fig. 2*A*). This suggests that the absence of PhTX sensitivity with PP stimulation in GluR1-S845A HM is unlikely due to a reduction in channel open probability, and support a loss of perisynaptic CP-AMPARs. Because of its sensitivity to GluR1-S845 mutation, our data also imply that the perisynaptic CP-AMPARs are likely GluR1 homomers.

To determine how the GluR1-S845 site affects perisynaptic CP-AMPARs, we examined whether the GluR1-S845A mutation has a global effect on the expression of GluR1. To do this, we first quantified the surface levels of AMPAR subunits using steady-state biotinylation of hippocampal slices (Fig. 2*B*). Surprisingly, GluR1-S845A HM expressed normal levels of surface GluR1 (WT: 45 ± 7.8% of total GluR1, $n = 7$; HM: 44 ± 7.7%, $n = 7$), but the surface GluR2 level was significantly increased (WT: 20 ± 4.2% of total GluR2, $n = 7$; HM: 52 ± 9.9%, $n = 7$; $P < 0.004$, t-test) (Fig. 2*B*). This resulted in about 60% reduction in the GluR1/GluR2 ratio on the cell surface (WT: 2.5 ± 0.38, $n = 7$; HM: 1.0 ± 0.18, $n = 7$; $P < 0.007$, t-test) (Fig. 2*B*). These changes were restricted to the plasma membrane, as there was no significant change in GluR1, GluR2, or the GluR1/GluR2 ratio in the total homogenates of GluR1-S845A HM (Fig. S1*C*). These results suggest that lacking the S845 site globally alters the GluR1/GluR2 ratio across the cell surface.

Because the lack of perisynaptic CP-AMPAR in the mutants did not correlate with a change in the surface GluR1 levels, we surmised that GluR1 homomers are replaced by GluR1/GluR2 heteromers. To determine this, we measured the GluR1 homomer level by quantifying GluR1 left after depleting GluR2/3-containing AMPARs. We immunoprecipiated GluR2/3 from hippocampal homogenates of wild-types and mutants using an antibody directed against the carboxy-terminal of GluR2/3. Under our conditions, less than 3% of GluR2/3 remained in the unbound supernatant fraction ($n = 7$). GluR1 in the unbound fraction was quantified as GluR1

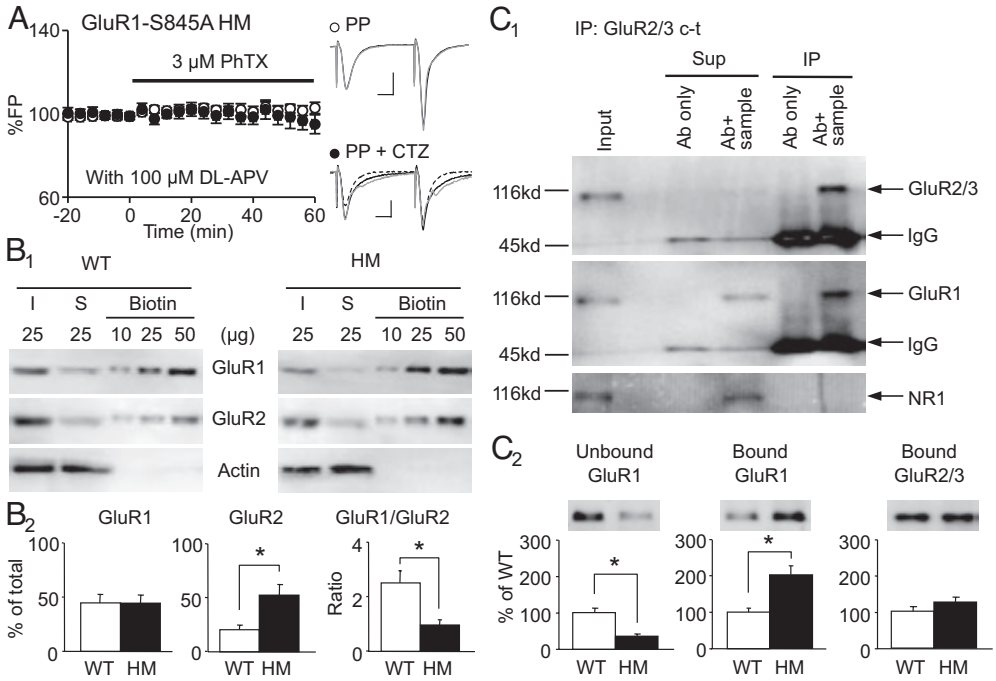

Fig. 2. Lack of perisynaptic CP-AMPARs in GluR1-S845A HM. (*A*) PhTX did not alter PP evoked AMPAR responses in GluR1-S845A homozygous (HM) mice with (filled circle) or without (open circle) 50 μM CTZ. Right, superimposed traces taken before (dotted gray line) and during CTZ application (black line), as well as 1 h post-PhTX (gray line). (Scale bar, 0.5 mV, 10 ms.) (B_1) Sample blots of steady-state biotinylation. Total (input, I), supernatant (S), and biotinylated surface proteins (Biotin) were loaded on the same gel for quantification. Specificity of surface labeling was verified by a lack of actin in the biotin lanes. (B_2) Quantification of surface GluR1 (left), GluR2 (middle), and GluR1/GluR2 ratio (right) in WT and HM. (C_1) Representative immunoblots for GluR2/3 immunoprecipitation (IP) experiments. The particular blot is of HM samples. Almost all GluR2/3 subunits were pulled down by the GluR2/3 c-terminal antibody, as seen from an absence of GluR2/3 signal in the supernatant (Sup) lane (top). GluR1 subunits left in the supernatant are likely GluR1 homomers (middle). The specificity of AMPAR pull-down is noted from a lack of NR1 in the IP fraction (bottom). (C_2) Quantification of GluR1 in unbound (left) and bound (IP, middle) fractions. Equivalent levels of GluR2/3 are pulled down in the IP fractions (right). *, $P < 0.01$.

homomers. In wild-types, about 17% of GluR1 existed as homomers ($n = 4$), which is similar to what has been reported before (≈19%) (30). We found that GluR1-S845A HM have significantly less GluR1 homomers than in wild-type littermates (WT: 100 ± 12.8% of average WT, HM: 36 ± 5.3%, $n = 10$ each; $P < 0.0001$, t-test) (Fig. 2*C*), and have about two times more GluR1 associated with GluR2/3 (WT: 100 ± 10.7% of average WT, HM: 199 ± 25.1%, $n = 10$ each; $P < 0.005$, t-test) (Fig. 2*C*). Our results suggest that the lack of perisynaptic CP-AMPARs in the GluR1-S845A HM is, at least in part, due to a cell-wide loss of GluR1 homomers and a concominant increase in the GluR1/GluR2 heteromers. The latter is further confirmed by our result that there are more GluR2 bound to GluR1 in the mutants (Fig. S2).

Inhibiting Lysosomal Protease Activity Restores Perisynaptic CP-AMPARs in the GluR1-S845A Mutants. To test whether the loss of perisynaptic CP-AMPARs in GluR1-S845A HM is due to lysosomal degradation, we incubated hippocampal slices with 50 μM leupeptin (a lysosomal protease inhibitor) for at least 2 h before testing the PhTX sensitivity of AMPAR responses. We found that leupeptin restored PhTX sensitivity in the mutants to a similar level seen in wild-types, while 10 μM MG-132 (a proteasome inhibitor) did not [HM control: 100 ± 6.3% of baseline 60 min post-PhTX, $n = 8$; HM + leupeptin: 81 ± 3.0%, $n = 7$; HM + MG-132: 94 ± 5.8%, $n = 7$; ANOVA: $F(2, 19) = 4.56$, $P < 0.03$, posthoc test: $P < 0.008$ between control and leupeptin group] (Fig. 3*A*). These results suggest that the assembly and surface insertion of GluR1 homomers still occur in the mutants, but the CP-AMPARs are degraded by lysosomes. Leupeptin did not significantly alter the PhTX sensitivity of AMPAR responses in wild-types (WT: 86 ± 2.0% of baseline 60 min post-PhTX, $n = 6$; WT + Leu: 86 ± 3.2%, $n = 7$) (Fig. 3*B*) indicating that perisynaptic CP-AMPARs are quite stable under basal conditions.

Loss of Perisynaptic CP-AMPARs Following Chemical Long-Term Depression (ChemLTD). Next we acutely dephosphorylated the S845 site by inducing chemLTD in wild-type hippocampal slices (31, 32) to see whether this can also remove CP-AMPARs. Similar to our previous study (32), chemLTD dephosphorylated S845, which lasted up to 2 h (Ctl: 100 ± 4.8%, 1 h: 68 ± 5.0%, 2 h: 72 ± 7.2%, $n = 8$ each; ANOVA: $F(2, 14) = 12.6$, $P < 0.001$) (Fig. 4*A*). We assessed PhTX sensitivity of AMPAR responses evoked by PP stimulation at 80 min after inducing chemLTD. ChemLTD abolished the PhTX sensitivity (With PhTX: 109 ± 5.5% of baseline renormalized to the average of 20 min preceeding PhTX application, $n = 7$; No PhTX: 110 ± 6.2% of renormalized baseline, $n = 8$) (Fig. 4*B*) suggesting that acute dephosphorylation of S845 in wild-types can remove perisynaptic CP-AMPARs.

Low Frequency Stimulation (LFS)-Induced LTD Is also Associated with a Loss of Perisynaptic CP-AMPARs. Similar to chemLTD, low frequency stimulation (LFS)-induced LTD is also accompanied by GluR1-S845 dephosphorylation (25). To test whether LFS-LTD can regulate perisynaptic CP-AMPARs, we performed a two-pathway experiment in hippocampal slices obtained from wild-type mice. We isolated two independent inputs converging onto the same population of CA1 neurons, as determined by a lack of cross-pathway facilitation (Fig. S3 *A* and *B*). After a stable baseline using alternating PP stimulations to both pathways, LFS (1 Hz, 15 min) was delivered to one pathway to induce LTD

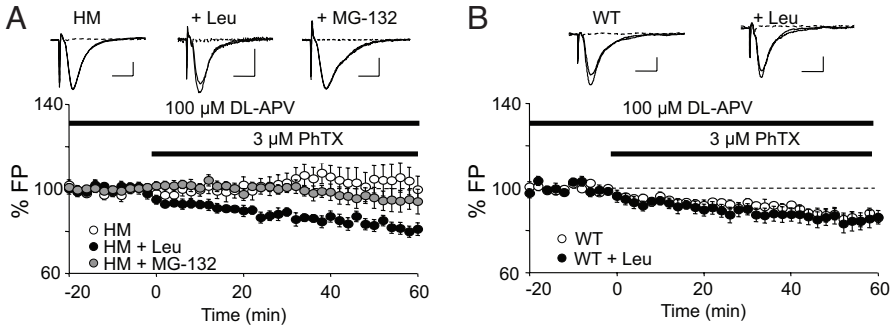

Fig. 3. Inhibiting lysosomal proteases restores perisynaptic CP-AMPARs in GluR1-S845A HMs. (*A*) In GluR1-S845A HM, preincubation with leupeptin, a lysosomal protease inhibitor, revealed PhTX sensitivity (black circles), but not preincubation with a proteosome inhibitor MG-132 (gray circles). (*B*) Leupeptin treatment in wild-type slices did not enhance PhTX sensitivity of AMPAR responses. Top panels: superimposed traces taken before and 1 h after PhTX, as well as after adding NBQX at the end of the experiment (dotted traces). (Scale bar, 0.25 mV, 10 ms.)

(LTD pathway). Stimulation in the other pathway (control pathway) was turned off for the duration of LFS. After LFS, PP stimulation was resumed in both pathways, and 100 μM APV was added to block NMDA receptors. Once responses in both pathways stabilized, 3 μM PhTX was applied to block CP-AMPARs. PhTX produced significantly less depression in the LTD pathway compared to the control pathway (CTL: 90 $\pm$ 2.4% of renormalized baseline measured 60 min after the onset of PhTX application; LTD: 93 $\pm$ 2.8%; $n = 14$; $P < 0.02$ between CTL and LTD, paired *t*-test) (Fig. 5). We verified that in the absence of PhTX, both control and LTD pathways are quite stable over the same period (Fig. S3*C*).

Discussion

We present evidence that CP-AMPARs, likely GluR1 homomers, are present at perisynaptic sites of the Schaffer collateral to CA1 inputs. These receptors are not normally activated but can be recruited under certain conditions, such as during PP stimulation and by glutamate spill-over induced by TBOA application. The stability of the perisynaptic CP-AMPARs was dependent on GluR1-S845 phosphorylation, which when absent promoted lysosomal degradation of the GluR1 homomers. Acute dephosphorylation of GluR1-S845, as during chemLTD and LFS-induced LTD, removed the perisynaptic CP-AMPARs. These results suggest that perisynaptic CP-AMPARs can be dynamically regulated by neural activity.

The majority of studies fail to detect CP-AMPARs at Schaffer collateral synapses on CA1 neurons under basal conditions (20, 21, 33, 34), but there are debates as to whether CP-AMPARs are detected following LTP induction. Some studies found that CP-AMPARs are expressed following LTP (21, 33–35), while others do not (20). A recent study suggests that LTP induction transiently incorporates CP-AMPARs at

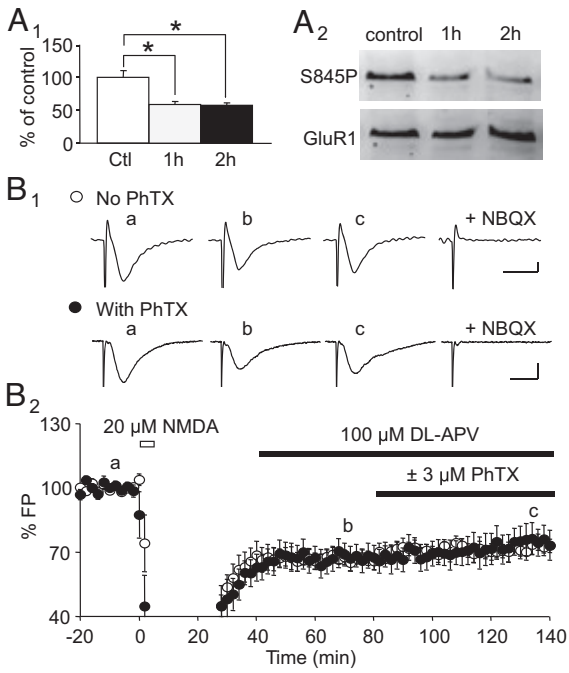

Fig. 4. Acute dephosphorylation of GluR1-S845 by chemLTD removes perisynaptic CP-AMPARs in wild-type mice. (A_1) ChemLTD induction caused a prolonged dephosphorylation of GluR1-S845. *, $P < 0.01$. (A_2) Sample blots showing GluR1-S845 phosphorylation (upper blot) and total GluR1 (lower blot). (B_1) Representative traces taken at times indicated in B_2. Addition of NBQX at the end of the experiment abolished the responses. (Scale bar, 0.25 mV, 10 ms.) (B_2) A brief application of NMDA (20 μM, 3 min) produced chemLTD of AMPAR responses, and abolished the PhTX sensitivity of PP evoked AMPAR responses (filled circles). Open circles: control chemLTD chased by 100 μM DL-APV without PhTX application.

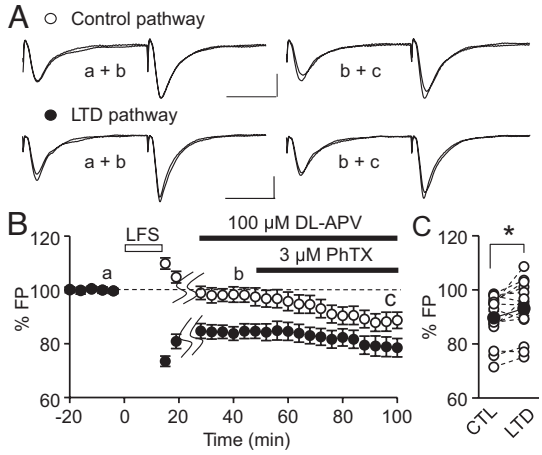

Fig. 5. LFS-induced LTD removes perisynaptic CP-AMPARs. (*A*) Representative traces taken at times indicated in *B*. (*B*) Alternating PP stimulation were given to two independent inputs converging on a group of CA1 neurons. One pathway received LFS to induce LTD (closed circles), while stimulation was turned off in the control pathway (CTL, open circles). After stabilization of synaptic responses after LFS, 3 μM PhTX was bath applied. (*C*) The responses after PhTX was renormalized to the average responses during the 20 min preceding PhTX application, and the averages of the last 10 min of CTL and LTD pathway from the same slice are plotted as a pair. *, $P < 0.03$.

perisynaptic sites (36). The latter study did not detect perisynaptic CP-AMPARs under basal conditions, but our results suggest otherwise. The reason for this discrepancy is unclear, but may be due to differences in age (P13–18 vs. P21–28) or species (rats vs. mice) used. Because we find that the perisynaptic expression of CP-AMPARs is linked to GluR1-S845 phosphorylation, differences in the state of neuromodulatory systems linked to PKA signaling may also influence the detection of CP-AMPARs. Our observation that PP stimulation reveals PhTX sensitivity of the first pulse response (Fig. 1*A*) is counterintuitive considering that the second stimulation pulse is most likely to activate perisynaptic AMPARs. We believe this indicates activity-dependent exchange or recruitment of perisynaptic CP-AMPARs to synaptic sites, because the PhTX sensitivity of the first pulse response of PP stimulation is blocked by a group 1 mGluR antagonist (100 μM AIDA) (Fig. S4*A*). Interestingly, PhTX applied in the presence of AIDA caused a small but a significant decrease in the PPF ratio (Fig. S4*A*), consistent with the idea that mostly perisynaptic CP-AMPARs are being blocked. AIDA application alone did not significantly alter the first pulse response or the PPF ratio (Fig. S4*B*). A recent study provided evidence in cerebellar stellate cells that mGluR activation promotes exchange of synaptic CP-AMPARs with GluR2-containing AMPARs (37). Whether this suggests a general role of group 1 mGluRs in regulating synaptic trafficking of CP-AMPARs awaits further investigation.

Our data suggest that GluR1-S845 stabilizes CP-AMPARs at perisynaptic sites by preventing lysosomal degradation of GluR1. This is consistent with other studies showing that dephosphorylation of the S845 site promotes endocytosis (18, 26, 27) and lysosomal degradation of GluR1 (27), while phosphorylation stabilizes GluR1 at dendrites (28). Interestingly, blocking lysosomal activity did not enhance PhTX sensitivity in wild-types, suggesting that the perisynaptic CP-AMPARs are not targeted to lysosomes under basal conditions. Considering a recent report that phosphorylation prevents lysosomal degradation of dendritic GluR1 (28), our data imply that CP-AMPARs are likely phosphorylated on the GluR1-S845 site. Acute dephosphorylation of this site, either by NMDA application or LTD induction, was required to remove the CP-AMPARs. The regulation of perisynaptic CP-AMPARs by LTD in our study is similar to what was reported for deconsolidation of LTP by LFS (36). This is interesting because LTD and deconsolidation of LTP, both of which are induced by LFS, are known to use distinct signaling [reviewed in (38)]. Collectively, these results suggest that the regulation of perisynaptic CP-AMPARs is a target of long-term synaptic depression mechanisms.

Unexpectedly, the lack of GluR1-S845 site upregulated GluR2, without changes in GluR1, at the cell surface. Taken together with the cell-wide loss of GluR1 homomers in GluR1-S845A HM, we infer that the GluR1 homomers are replaced by GluR1/GluR2 heteromers. However, we also found that the current-voltage (I-V) curve of AMPAR-EPSCs is supralinear in the GluR1-S845A HM when compared to the wild-type littermates (Fig. S5*A*). This suggests that there is an increase in the level of GluR2 at synapses, as AMPARs with high content of GluR2 exhibit outward rectifying current (39). Consistent with this idea, the level of GluR2 in the PSD fractions of GluR1-S845A HM was elevated (Fig. S1*B*). This is not likely a side-effect of mutating the S845 site, because acute dephosphorylation of S845 by chemLTD was also associated with an outward rectifying AMPAR current (Fig. S5*B*). Our results imply that removing perisynaptic GluR1 homomers may be linked to an upregulation of GluR2 at synapses.

Based on our results we propose a model (Fig. S6) in which perisynaptic CP-AMPARs are regulated by GluR1-S845 phosphorylation. The main role of the S845 is to prevent lysosomal degradation of the CP-AMPARs. Previous studies in C. elegans have demonstrated that the endocytosis of glr1, the GluR1 homologue, is regulated by monoubiquination (40). Monoubiquination commonly regulates endocytosis of membrane proteins and targets the monoubiquinated protein for lysosomal degradation (41). As phosphorylation has previously been show to regulate the association of E3 ubiquitin ligases with substrates (41), it is tempting to speculate that S845 phosphorylation may regulate the interaction of GluR1 with an E3 ubiquitin ligase and thus regulate its endocytosis, ubiquination, and lysosomal degradation. In any case, the stable expression of CP-AMPARs at perisynaptic sites under basal conditions suggests that they can be recruited by repetitive high frequency input activity, as exemplified by the PP stimulation. This implies that the postsynaptic signaling will vary depending on the pattern of input activity. The removal of CP-AMPARs from perisynaptic locations following LTD is then expected to have functional consequences as to how the repetitive input activity impacts postsynaptic signaling.

Materials and Methods

Slice Preparation and Recordings. Acute hippocampal slices were prepared from P21–28 mice (wild-type and S845A HM) and recordings were done as described in *SI Text*.

Steady-State Surface Biotinylation. Hippocampus slices (400 μm thick) lacking the CA3 area were prepared according to the methods listed in *SI Text*. Surface proteins were biotinylated and pulled down using a standard procedure and quantified as detailed in *SI Text*.

Co-Immunoprecipitation (CoIP). The whole hippocampal tissues were collected, and co-IPs were done using a standard procedure detailed in *SI Text*.

Statistical Analysis. All data are expressed as mean ± SEM. Unpaired or paired Student's *t*-test or one-factor ANOVA followed by Fisher's PLSD posthoc tests were used as appropriate to determine statistical significance between groups. $P < 0.05$ were taken as significant.

ACKNOWLEDGMENTS. This work was supported by National Insitutes of Health Grant R01-EY014882 and a University of Maryland (UMD) Seed Grant (to H.-K.L.), a University of Maryland Anne Wiley Dissertation Fellowship (to K.H.), a University of Maryland Program in Neuroscience and Cognitive Science Summer Internship (to J.G.), and the Howard Hughes Medical Institute (to R.L.H.).

1. Shepherd JD, Huganir RL (2007) The cell biology of synaptic plasticity: AMPA receptor trafficking. *Annu Rev Cell* Dev Biol 23:613–643.
2. Seeburg PH, Higuchi M, Sprengel R (1998) RNA editing of brain glutamate receptor channels: Mechanism and physiology. *Brain Res Brain Res Rev* 26:217–229.
3. Liu SJ, Zukin RS (2007) Ca2+-permeable AMPA receptors in synaptic plasticity and neuronal death. *Trends Neurosci* 30:126–134.
4. Liu SJ, Cull-Candy SG (2005) Subunit interaction with PICK and GRIP controls Ca2+ permeability of AMPARs at cerebellar synapses. *Nat Neurosci* 8:768–775.
5. Gardner SM, et al. (2005) Calcium-permeable AMPA receptor plasticity is mediated by subunit-specific interactions with PICK1 and NSF. *Neuron* 45:903–915.
6. Liu B, et al. (2006) Ischemic insults direct glutamate receptor subunit 2-lacking AMPA receptors to synaptic sites. *J Neurosci* 26:5309–5319.
7. Bellone C, Luscher C (2006) Cocaine triggered AMPA receptor redistribution is reversed in vivo by mGluR-dependent long-term depression. *Nat Neurosci* 9:636–641.
8. Conrad KYT, Uejima JL, Reimers JM, Heng L-J, Shaham Y, Marinelli M, Wolf ME (2008) Formation of accumbens GluR2-lacking AMPA receptors mediates incubation of cocaine craving. *Nature* 454:118–121.
9. Goel A, et al. (2006) Cross-modal regulation of synaptic AMPA receptors in primary sensory cortices by visual experience. *Nat Neurosci* 9:1001–1003.
10. Sutton MA, Schuman EM (2006) Dendritic protein synthesis, synaptic plasticity, and memory. *Cell* 127:49–58.
11. Thiagarajan TC, Lindskog M, Tsien RW (2005) Adaptation to synaptic inactivity in hippocampal neurons. *Neuron* 47:725–737.
12. Aoto J, Nam CI, Poon MM, Ting P, Chen L (2008) Synaptic signaling by all-trans retinoic acid in homeostatic synaptic plasticity. *Neuron* 60:308–320.
13. Roche KW, O'Brien RJ, Mammen AL, Bernhardt J, Huganir RL (1996) Characterization of multiple phosphorylation sites on the AMPA receptor GluR1 subunit. *Neuron* 16:1179–1188.

14. Banke TG, et al. (2000) Control of GluR1 AMPA receptor function by cAMP-dependent protein kinase. *J Neurosci* 20:89–102.
15. Esteban JA, et al. (2003) PKA phosphorylation of AMPA receptor subunits controls synaptic trafficking underlying plasticity. *Nat Neurosci* 6:136–143.
16. Oh MC, Derkach VA, Guire ES, Soderling TR (2006) Extrasynaptic membrane trafficking regulated by GluR1 serine 845 phosphorylation primes AMPA receptors for long-term potentiation. *J Biol Chem* 281:752–758.
17. Gao C, Sun X, Wolf ME (2006) Activation of D1 dopamine receptors increases surface expression of AMPA receptors and facilitates their synaptic incorporation in cultured hippocampal neurons. *J Neurochem* 98:1664–1677.
18. Man HY, Sekine-Aizawa Y, Huganir RL (2007) Regulation of {alpha}-amino-3-hydroxy-5-methyl-4-isoxazolepropionic acid receptor trafficking through PKA phosphorylation of the Glu receptor 1 subunit. *Proc Natl Acad Sci USA* 104:3579–3584.
19. Seol GH, et al. (2007) Neuromodulators control the polarity of spike-timing-dependent synaptic plasticity. *Neuron* 55:919–929.
20. Adesnik H, Nicoll RA (2007) Conservation of glutamate receptor 2-containing AMPA receptors during long-term potentiation. *J Neurosci* 27:4598–4602.
21. Plant K, et al. (2006) Transient incorporation of native GluR2-lacking AMPA receptors during hippocampal long-term potentiation. *Nat Neurosci* 9:602–604.
22. Bowie D, Mayer ML (1995) Inward rectification of both AMPA and kainate subtype glutamate receptors generated by polyamine-mediated ion channel block. *Neuron* 15:453–462.
23. Kamboj SK, Swanson GT, Cull-Candy SG (1995) Intracellular spermine confers rectification on rat calcium-permeable AMPA and kainate receptors. *J Physiol* 486:297–303.
24. Mosbacher J, et al. (1994) A molecular determinant for submillisecond desensitization in glutamate receptors. *Science* 266:1059–1062.
25. Lee HK, Barbarosie M, Kameyama K, Bear MF, Huganir RL (2000) Regulation of distinct AMPA receptor phosphorylation sites during bidirectional synaptic plasticity. *Nature* 405:955–959.
26. Lee HK, et al. (2003) Phosphorylation of the AMPA receptor GluR1 subunit is required for synaptic plasticity and retention of spatial memory. *Cell* 112:631–643.
27. Ehlers MD (2000) Reinsertion or degradation of AMPA receptors determined by activity-dependent endocytic sorting. *Neuron* 28:511–525.
28. Kessels HW, Kopec CD, Klein ME, Malinow R (2009) Roles of stargazin and phosphorylation in the control of AMPA receptor subcellular distribution. *Nat Neurosci* 12:888–896.
29. Partin KM, Fleck MW, Mayer ML (1996) AMPA receptor flip/flop mutants affecting deactivation, desensitization, and modulation by cyclothiazide, aniracetam, and thiocyanate. *J Neurosci* 16:6634–6647.
30. Wenthold RJ, Petralia RS, Blahos J, II, Niedzielski AS (1996) Evidence for multiple AMPA receptor complexes in hippocampal CA1/CA2 neurons. *J Neurosci* 16:1982–1989.
31. Kameyama K, Lee HK, Bear MF, Huganir RL (1998) Involvement of a postsynaptic protein kinase A substrate in the expression of homosynaptic long-term depression. *Neuron* 21:1163–1175.
32. Lee HK, Kameyama K, Huganir RL, Bear MF (1998) NMDA induces long-term synaptic depression and dephosphorylation of the GluR1 subunit of AMPA receptors in hippocampus. *Neuron* 21:1151–1162.
33. Guire ES, Oh MC, Soderling TR, Derkach VA (2008) Recruitment of calcium-permeable AMPA receptors during synaptic potentiation is regulated by CaM-kinase I. *J Neurosci* 28:6000–6009.
34. Lu Y, et al. (2007) Age-dependent requirement of AKAP150-anchored PKA and GluR2-lacking AMPA receptors in LTP. *EMBO J* 26:4879–4890.
35. Bagal AA, Kao JP, Tang CM, Thompson SM (2005) Long-term potentiation of exogenous glutamate responses at single dendritic spines. *Proc Natl Acad Sci USA* 102:14434–14439.
36. Yang Y, Wang XB, Frerking M, Zhou Q (2008) Delivery of AMPA receptors to perisynaptic sites precedes the full expression of long-term potentiation. *Proc Natl Acad Sci USA* 105:11388–11393.
37. Kelly L, Farrant M, Cull-Candy SG (2009) Synaptic mGluR activation drives plasticity of calcium-permeable AMPA receptors. *Nat Neurosci* 12:593–601.
38. Lee HK, Huganir RL (2008) AMPA receptor regulation and the reversal of synaptic plasticity–LTP, LTD, depotentiation, and dedepression. *Learning and Memory: A Comprehensive Reference*, ed Sweatt JD (Elsevier press), Vol 4.
39. Verdoorn TA, Burnashev N, Monyer H, Seeburg PH, Sakmann B (1991) Structural determinants of ion flow through recombinant glutamate receptor channels. *Science* 252:1715–1718.
40. Burbea M, Dreier L, Dittman JS, Grunwald ME, Kaplan JM (2002) Ubiquitin and AP180 regulate the abundance of GLR-1 glutamate receptors at postsynaptic elements in C. elegans. *Neuron* 35:107–120.
41. Haglund K, Di Fiore PP, Dikic I (2003) Distinct monoubiquitin signals in receptor endocytosis. *Trends Biochem Sci* 28:598–603.